Icarus 311 (2018) 105–112

Contents lists available at ScienceDirect

Icarus

journal homepage: www.elsevier.com/locate/icarus

Constraining the parameter space of comet simulation experiments

Erika Kaufmann[1], Axel Hagermann[1,*]

The Open University, Walton Hall, Milton Keynes MK7 6AA, United Kingdom

ARTICLE INFO

Article history:
Received 17 January 2018
Revised 7 March 2018
Accepted 27 March 2018
Available online 28 March 2018

Keywords:
Comet analogues
Comet simulation experiments
Dusty ice
Laboratory
Surfaces
Hardness
Porous ices

ABSTRACT

Our interpretation of the data returned by Rosetta and other cometary missions is based on the predictions of theoretical models and the results of laboratory experiments. For example, Kossacki et al. (2015) showed that 67P's surface hardness reported by Spohn et al. (2015) can be explained by sintering. The present work supports Rosetta's observations by investigating the hardening process of the near-surface layers and the change in surface morphology during insolation. In order to create as simple an analogue as possible our sample consists of pure, porous H_2O ice and carbon black particles. The observations suggest that translucence of the near-surface ice is important for enabling subsurface hardening. As an end product of our experiments we also obtained carbon agglomerates with some residual strength.

1. Introduction

The space missions Giotto, Deep Space I, Stardust, Deep Impact, EPOXI and, most recently, Rosetta have substantially contributed to our understanding of the processes driving the activity of comets. Especially Rosetta and its lander Philae obtained information on 67P/Churyumov–Gerasimenko (hereafter 67P) on unprecedented scales, observing from orbit and on the surface of the nucleus.

The Rosetta mission also marks the first time that a detailed map of a comet nucleus could be generated. Images of comet 67P taken by the OSIRIS imaging system (Keller et al., 2007) show a wide variety of different structures and textures. This includes dust-covered terrains, smooth terrains, 'brittle' materials with pits and circular structures, large-scale depressions, and exposed consolidated surfaces (El-Maarry et al., 2015; Thomas et al., 2015). Higher resolution OSIRIS data also gave evidence of bright icy outcrops on the surface of 67P (Pommerol et al., 2015). These meter-sized bright spots are widespread on the surface within the different areas.

As discussed by Barucci et al. (2016) the detection of the spectral signatures of H_2O ice in these bright spots confirms that they are icy. In their studies they compared 13 of the bright spots identified by OSIRIS with data obtained by the VIRTIS instrument (Coradini et al., 2007). Eight of them show clear evidence of H_2O ice in their spectra, with a surface water content reported to range from 0.1% to 7.2%. Bright spots could also be observed at other periodic comets. For example Comet 9P/Tempel 1 (Sunshine et al., 2006) and 103P/Hartley 2 (Li et al., 2013) also revealed the presence of intriguing bright spots on their surfaces.

Some data collected by the various Rosetta instruments warrants further investigation by laboratory experiments: The evidence of surface water ice in active regions whilst large parts of the nucleus surface remain covered in dark dust has puzzled researchers since the Giotto days. Moreover, the morphology of the nucleus surface raises questions which physical processes might lead to the shaping of, e.g., the layer-like surface features or smooth-floored pits (Birch, 2017).

A number of comet simulation experiments have helped improve our understanding of the physics that drives cometary activity and thereby shapes cometary nuclei. The KOSI campaign (KOmeten SImulation, i.e. comet simulation) of the late 1980 s to early 1990 s was one of the largest and possibly most ambitious campaigns. KOSI was prompted by the appearance of comet 1P/Halley and the Giotto mission in 1986 and supported the design of the Rosetta mission. A review of the main results and their critical analysis can be found, for example in Lämmerzahl et al. (1995), Kochan et al. (1998) and Sears et al. (1999). KOSI included 11 large scale experiments and several small scale experiments (e.g. Kömle et al., 1996). Although those experiments provided crucial new insights into the physics and morphology of cometary analogue materials, the set-up was very complex. Moreover, several experimental parameters were changed at any given time, which makes it difficult to analyse all results in a quantitative manner.

* Corresponding author.
E-mail address: axel.hagermann@stir.ac.uk (A. Hagermann).
[1] Now at University of Stirling, Stirling, FK9 4LA.

https://doi.org/10.1016/j.icarus.2018.03.025

In order to minimize these difficulties and to create a solid experimental foundation for further theoretical investigations, a change in experimental scale took place, with small-scale experiments performed under conditions approximating those in the environment of cometary nuclei, focusing on phenomena that had not been directly or fully addressed in previous experiment campaigns. Gundlach et al. (2011) investigated the temperature dependent sublimation properties of hexagonal water ice and the gas diffusion through a dry dust layer covering the ice surface. Brown et al. (2012) investigated the characteristics of ice sublimation. The influence of a small amount of dissolved minerals on the temperature dependence of the sublimation coefficient of ice was investigated by Kossacki and Leliwa-Kopystynski (2014). Pommerol et al. (2011, 2015) and Poch et al. (2016) focus on the characterisation of the visible spectrophotometric properties of analogues of solar system icy surfaces with comets as a key aspect.

Small-scale experiments involving less complexity than the simulations of the KOSI era allow us to isolate the key parameters and processes involved in cometary activity. In order to investigate solar light absorption by a porous dust-ice mixture, a series of experiments was carried out in the Open University's Planetary Ices Laboratory. Our model comet consisted of only two ingredients: H_2O ice and carbon particles (carbon black). These samples were irradiated for several hours, temperature and hardness profile were measured and the change of the surface structure recorded. The dependence of sample evolution on subsurface solar light absorption by dark admixtures to the ice was studied by varying quantities of carbon particles added to the porous H_2O ice. Against the backdrop of the Rosetta's observations, showing a comet that, in terms of composition, appears to be more of a slightly icy rubble pile than a dirty snowball, our samples may seem like a poor analogue because they consist almost entirely of water ice. However, the purpose of our experiments is not to simulate as accurate a comet analogue as possible; this is what the KOSI experiments did, informed (and constrained) by the state of knowledge at the time. Instead, our aim is to understand the origin and mechanisms cometary activity: where energy is absorbed, how dust ejection is achieved and how the physical properties of the icy component of a comet changes. This is best investigated using a simple setup like ours. Our setup ensures efficient absorption of solar radiation at depth by the carbon particles whilst maintaining translucence of the ice.

2. Laboratory experiments

The set-up for our experiment was as follows: a cylindrical container consisting of two Perspex half shells (inner diameter of the container $d = 12.4$ cm) was installed on a nitrogen-cooled base plate inside an environmental chamber. The base plate was pre-cooled to an initial temperature T_0 while the chamber was depressurised. After the base plate had reached T_0, the chamber was opened, the container filled with the sample material and the chamber was then closed and depressurised again. The sample was cooled until the temperature gradient inside it had stabilised. Then the sample was irradiated using a Solar Simulator with an AM0 filter for several hours. During the irradiation phase T_0 was kept constant and the temperature profile inside the sample was measured using a vertical array of RTD sensors (PT100) with a spacing of 1 cm, starting 1 cm from the base plate. Additionally, a time-lapse record of the morphology of the sample during the irradiation phase was obtained using a set of commercial off-the-shelf webcams.

The ice for the samples was produced by spraying deionized water into LN_2 using a commercial spray gun. In doing so the droplets froze out immediately and settled at the bottom of the Dewar to form a loose aggregate of small spherical particles. These ice particles were subsequently sieved which led to samples including grain sizes of $d_{ice} \leq 1.0$ mm, with a random size distribution within that range. A small amount of carbon particles (carbon black CAS# 1333-86-4, $d_c \leq 300$ nm) by weight was added to the ice grains and mixed by stirring. Carbon black was chosen to obtain a darker material whilst trying to keep the composition of the mixture as simple and chemically inert as possible and therefore a low albedo like observed at comets. The hardness of this basic granular mix is about 4–6 kPa. For comparison, the surface hardness of freshly fallen snow can range from 2.5 kPa to 10 kPa (Pomeroy and Brun, 2001).

Hardness was measured using the method described by Poirier et al. (2011). In their method, a ball is dropped from a known height onto the sample. Hardness is then calculated from the kinetic energy of the impactor and the volume of the impact crater formed. Poirier et al.'s method effectively measures dynamic hardness which, according to Epifanov (2004) translates into ultimate tensile strength divided by 0.383. In order to obtain the best results, we gradually varied the size of the balls (16.5–32.7 mm), their density (we used wood, glass, metal), and the drop height (300–426 mm), depending on sample hardness. Although this method is more accurate than using a handheld field penetrometer, a measurement error of up to 20% remains (Grabowski, O. private communication).

The samples in our experiments were $h_0 = 15$ cm high, with a density of $\rho = 461 \pm 66$ kg/m^3. Using $\rho = 917$ kg/m^3 for the density of water ice (e.g. Steiner et al., 1991), this translates directly into a corresponding porosity of $\varphi = 0.5 \pm 0.07$. This value is comparable to the density of 470 ± 45 kg/m^3 of 67P reported e.g. by Sierks et al. (2015).

The temperature of the base plate was set to $T_0 = 173$ K. Whilst the initial conditions were left unchanged for the entire series of experiments, the percentage of carbon added was varied between 0.02% and 0.5%. The samples were irradiated for 18 hours with an insolation intensity of approximately 650 W/m^2.

Strictly speaking, insolation intensity does not remain constant during the experiments as shadowing effects occur for two reasons. Firstly, water condensate on the view port results in reduction of insolation over a small area (usually the centre) of the view port for the first 15 to 20 minutes. Secondly, the view port loses some transparency as the carbon particles ejected from the sample start to adhere to its inner surface. Over the entire irradiation phase this leads to a reduction of the insolation provided to the sample surface. For our initial experiments up to 0.2% carbon black, we monitored the loss of intensity with a photodiode placed next to the sample and found an intensity loss between 10.6% and 12%, so we do not expect the decrease of intensity to have a large influence on our results. The particles are evenly distributed across the viewport, therefore the reduction of incoming irradiation is constant over the sample surface (Fig. 1) .

3. Results

A summary of the experiments is given in Table 1. As expected, the height of the samples decreases as surface ice is lost by sublimation. In terms of sample height, ice loss is largely constant although there is a small increase in ice loss between 0.1% and 0.5% (which might be expected, as higher carbon content implies more effective absorption of solar radiation).

3.1. Hardness

The results of the hardness measurements are given in Fig. 2, where the initial observation of an activity peak around 0.2% carbon is mirrored: Samples with 0.2% and 0.3% carbon show the greatest increase in hardness, in particular at a depth of approx.

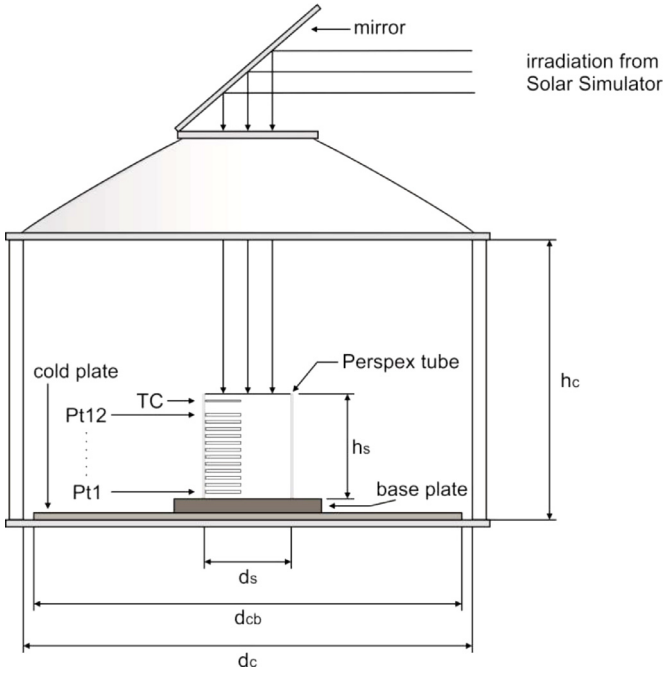

Fig. 1. Schematic of laboratory experiment setup.

6 cm. Higher carbon content appears to prevent ice hardening at depth.

3.2. Temperature profiles

Ice hardening under our experimental conditions occurs by sintering. In order to understand the sintering process, and thereby hardness, we need to examine the temperature profiles as measured inside the samples, which are given in Fig. 3.

We note that temperature profiles at depth after irradiation are very similar. While the base temperatures are identical, temperatures in the sample between 4 cm above the base and 1 cm below the surface are restricted to a narrow range of 205 ± 5 K. Comparing our temperature profiles with Steiner et al. (1991) simple theoretical model suggests that energy transport by conduction is almost negligible. Assuming that advection transports heat from the point of ice sublimation to the point of ice deposition, we would expect a linear temperature profile (at least for the 'dark' and very

Table 1
Values for the maximum hardness P_{max} at distance d from the surface for the different amounts of carbon particles pc. The decrease in sample thickness over 18 hours of radiation Δz, i.e. distance between the initial sample height and the final ice surface is measured along the z-axis. The error of the hardness values is about ± 20%.

Nr.	pc (%)	P_{max} (kPa)	d (cm)	Δz (cm)
1	0.02	102.9	3.5	3.0
2	0.1	115.9	2.9	2.5
3	0.2	163.5	6.5	2.4
4	0.3	121.2	6.5	2.5
5	0.4	42.5	6.3	3.0
6	0.5	48.7	6.0	3.0

transparent samples where no mass transfer manifests itself in an increase in sample hardness. We interpret the near-isothermal temperature profile throughout most of the sample depth, combined with the steep temperature drop near the base plate to imply that convection plays a dominant role in the energy transfer. In this context needs to be noted that most theoretical models such as Steiner et al. do not consider the influence of light absorption at depth.

3.3. Surface morphology

Our experiments show that sample hardness changes considerably with the amount of carbon added to the ice. In addition, significant changes of the sample's surface morphology were observed during the irradiation process. Figs. 4 and 5 demonstrate the visible change in sample surface morphology due to irradiation. At the start of the irradiation phase, the surface is light grey (depending on the amount of carbon added). After 18 hours of irradiation, carbon agglomerates have accreted on the sample surface. The structure of surface carbon agglomerates is highly dependent on carbon content: the higher the carbon content, the larger the agglomerates.

The first changes of the sample surface can already be observed within the first few minutes of the irradiation phase. During depressurisation a thin, homogeneous layer of carbon black accumulates on top of the sample. Particles are emitted immediately after irradiation has started. Within the first minute this affects only small particles, leading to a change of the surface that cannot be seen on the time-lapse recordings. However, it can be observed that these small particles settle at the view port of the chamber.

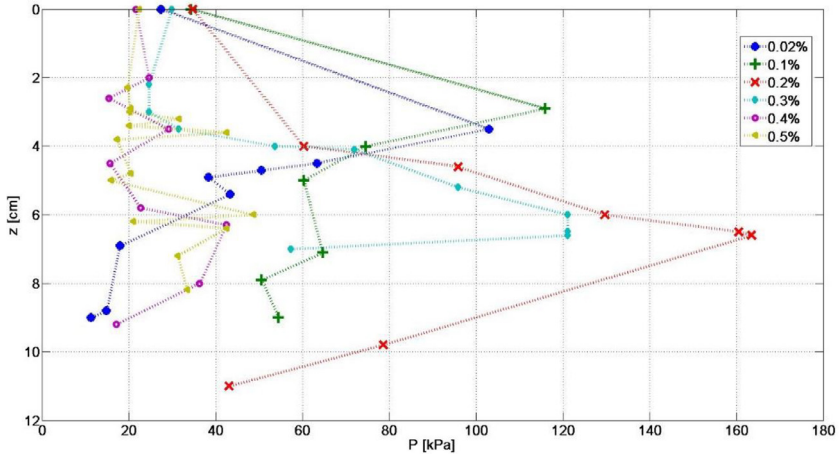

Fig. 2. Hardness values for different H_2O/carbon mixtures from the surface $z = 0$ down to the bottom of the sample. In order of increasing carbon content, the data points are averages from 2, 1, 2, 2, 3 and 2 experimental runs, respectively. Hardness of a fresh, unconsolidated sample is between 4 and 6 kPa.

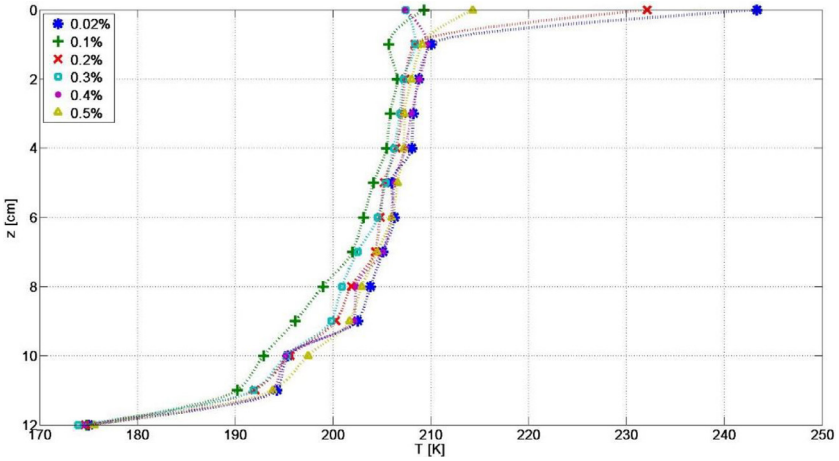

Fig. 3. Temperature profiles after 18 hours of irradiation. Zero depth is set to a height of 12 cm above the base plate. This is to enable a comparison between temperature and hardness measurements. As the sample shrinks during the irradiation phase, the topmost temperature sensor is no longer covered by ice, therefore temperature values measured closest to the initial surface are not included is no longer covered by the sample material at the end of the irradiation phase. Temperatures are unusually high for the sensors at $z = 0$ with 0.02% and 0.2% carbon because, at the time of measurement, sensor and/or cable are already directly exposed to solar irradiation. (For interpretation of the references to colour in this figure legend, the reader is referred to the web version of this article.)

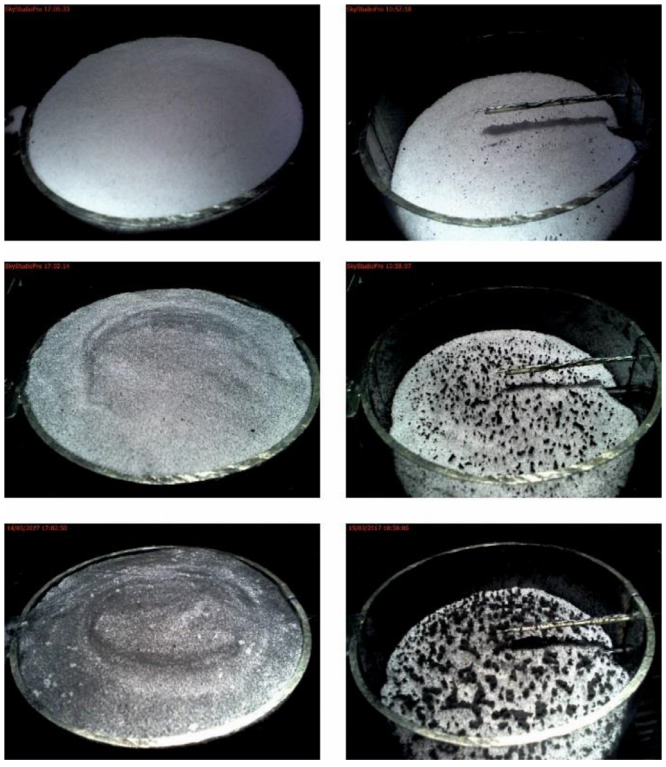

Fig. 4. Sample surface before (left) and after (right) 18 hours of irradiation. Each row shows examples of the results for different amounts of carbon. From top to bottom: 0.02%, 0.1%, and 0.2% of carbon black.

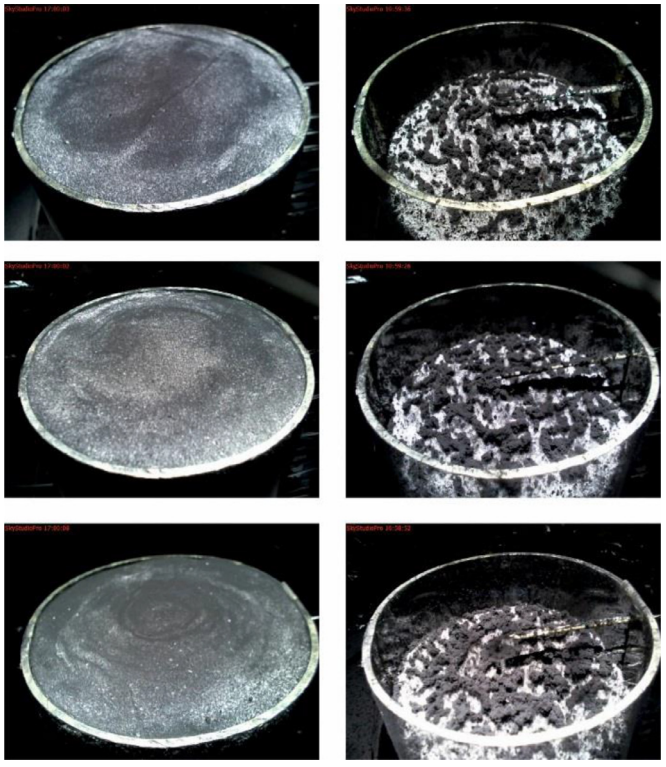

Fig. 5. Surface structure before (left) and after (right) 18 hours of irradiation. Top: 0.3%; second row: 0.4%; bottom: 0.5% carbon black. $T_0 = 173$ K, $h_0 = 15$ cm.

For the following few minutes, the sample surface brightens as patches of carbon particles are lifted. After some time (10 to 40 minutes, depending on the amount of carbon added) agglomerates can be seen to accrete. The time between the onset of irradiation and the time it takes for the clean sample surface to be fully exposed depends on carbon content: the more carbon black is added, the sooner the sample surface reaches maximum brightness. Although the image resolution of our web cams is insufficient for a reliable time estimate, the surface appears to be brightest 30–40 min after insolation start for 0.1% carbon, whereas it only takes about 25 min for a sample with 0.2% carbon to reach a similar state.

Although all samples show a noticeable surface change and a similar behaviour within the first minutes, the most distinct change can be observed with 0.5% carbon added. For approximately one minute there is hardly any change on the surface that is visible with the naked eye. Once the surface has been warmed, small bright spots start to appear randomly across the surface. After approximately two minutes of irradiation larger bright spots

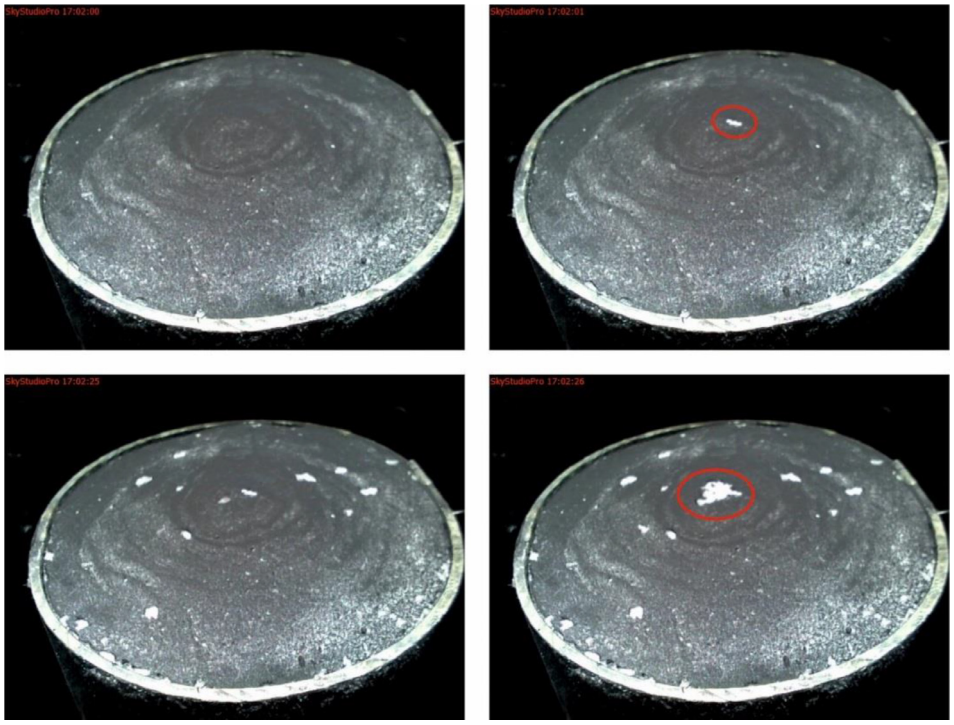

Fig. 6. Snapshots of the surface of a sample with 0.5% carbon. The upper left image was taken after 2 minutes of irradiation, the upper-right image one second later. The lower images were taken 24 (left) and 25 (right) seconds later. The marked bright spots are roughly estimated to have areas of about 15 mm^2 and 90 mm^2, respectively. Typical chamber pressures during insolation are around 6×10^{-5} mbar.

with areas up to 90 mm^2 show up (see Fig. 6). These spots have irregularly shaped boundaries and seem to be caused by patches or clusters of carbon dust (as opposed to individual particles) lifted off the surface. This implies that the dark layer initially accumulated on top of the sample is thin enough for the insolation to penetrate to the ice-rich sample below and cause sublimation. The layer is also fragile enough to be removed by the vapour pressure of the subliming water ice.

After about 10 minutes the surface is brighter than initially, with only a few dark speckles, some exhibiting needle-like structures. Further irradiation of the sample causes carbon agglomerates to grow.

The recordings also show that even after several hours of irradiation, the surface is still active and bigger agglomerates are moved. For example, they can be seen rolling across the surface, being pushed along by the ejected gas, or lifted into a more upright position. Some of the smaller agglomerates (estimated volume of up to 60 mm^3) can even be ejected from the sample, although some fall back onto the sample. In case of a low carbon amount some of the agglomerates are set into a vibrating motion by the gas ejected from the ice below.

With only a minor amount of carbon (0.02%) added to the ice, the surface structure hardly chances, only a few small agglomerates build up during the irradiation phase. However, bright spots can be observed on the surface for all H_2O/carbon mixtures.

The agglomerates of carbon particles that accumulate during the irradiation phase can reach heights of up to 5 mm if carbon content is as high as 0.5%. Samples of those surface agglomerates were collected after some of the experiments. Their structure showed remarkable mechanical strength: the carbon particles still stuck together and the agglomerates kept their shape when taken of the surface and allowed to dry. An example is shown in Fig. 7. The carbon agglomerates have a very low density of about 23 kg/m^3.

3.4. Dust dynamics

The ejection of individual particles can be observed in the side view time lapse recordings. Some of this particles/clusters are lifted nearly vertically from the surface, others have a parabolic trajectory. An example of particle ejection at a carbon content of 0.4% is shown in Fig. 8.

This effect can be observed for any amount of carbon - for the smallest amount the change in surface brightness is hard to recognize but same as for the other mixtures, the growing of agglomerates can be recorded and particles settle on the viewport.

The sample surface is active until the irradiation stops, particle emission can be observed throughout the irradiation phase. Even after several hours of irradiation agglomerates with diameters of approximately 1 to 1.5 mm can be emitted, a similar size as observed in some of the KOSI experiments (see e.g. Markiewicz et al., 1991). The carbon particles spread all over the chamber, smaller particles settle on the base plate, the walls, and on the viewport which is approximately 35 cm above the sample surface. Larger particles or agglomerates are lifted but fall back on the sample or the area close to the sample.

We estimate the gas drag of the vapour ejected from the sample, following the approach described by Grün et al. (1993) and assuming that the whole sample surface emits gas uniformly.

Consider a particle of radius r exposed to a flow of vapour of gas mass density ρ_g. The gas flow exerts a drag force F_D on the particle, which can be written as

$$F_D = \pi r^2 \frac{C_D}{2} \rho_g v_{cm}^2$$

where C_D the drag force coefficient, and $v_{cm} = \pi < v > /4$ with $< v >$ the average thermal speed. In order to lift particles, F_D needs to

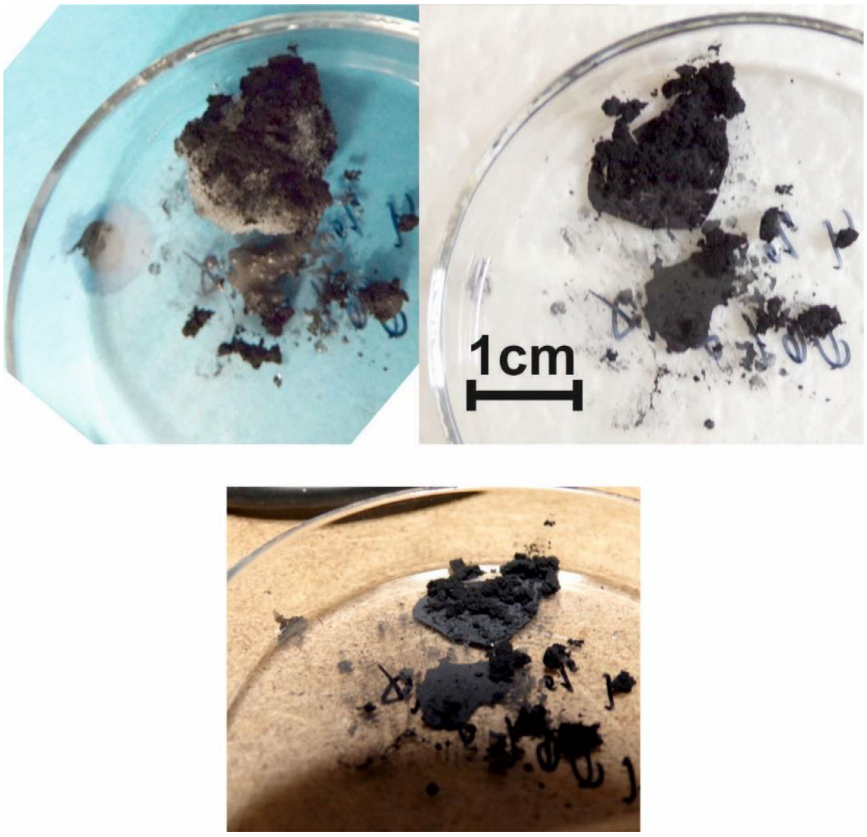

Fig. 7. Images from agglomerates built up during an experiment with a 0.4% sample. Upper left: image taken after the agglomerate was taken of the surface. Upper right: same agglomerate after drying. Lower image: same agglomerate, dried, image taken from a different angle.

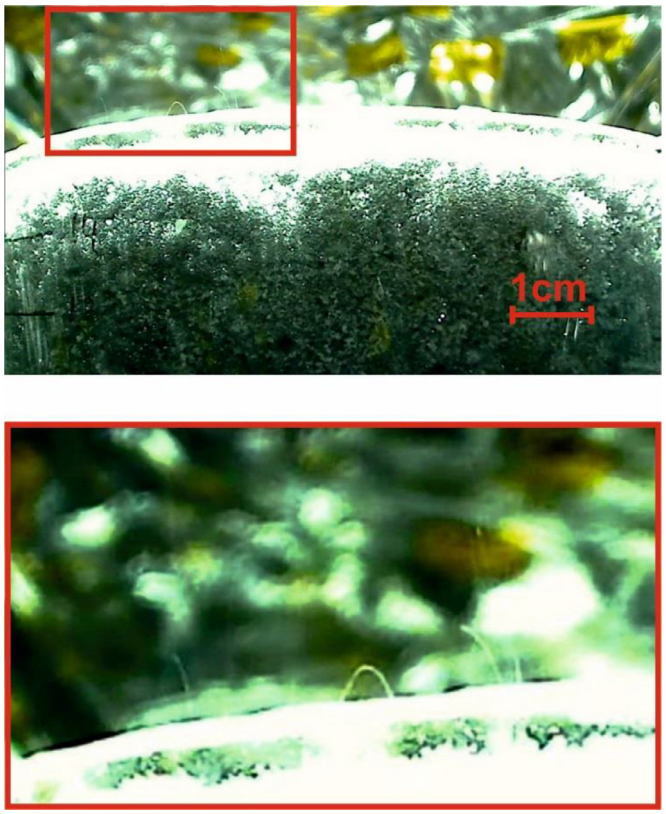

Fig. 8. Snapshot of particle ejection, example for a carbon content of 0.4%. Red rectangle: magnification 1:2.65.

exceed the gravitational force

$$F_G = \frac{4}{3}\pi r^3 \rho_d g,$$

with ρ_d the mean dust particle density and g the gravitational acceleration.

The vapour is assumed to be an ideal gas and therefore the gas density can be derived from the ideal gas law in its form $p = k/m\rho_g\ T$, where m is the molecular weight of water and k is the Stefan-Boltzmann constant. Assuming that the surface is a flat, homogeneously irradiated area that has warmed up to the sublimation temperature T_s, the upper boundary conditions are $T = T_s$ and the pressure p equals the saturation pressure $p_s(T_s)$ (see e.g. Benkhoff and Spohn, 1991).

With these assumptions one can estimate the force ratio $\gamma = F_D/F_G$ for the original, small carbon particles ($r = 150$ nm, $\rho_d = 1900\,\mathrm{kg/m^3}$) as well as for the agglomerates ($r = 0.5$ mm, $\rho_d = 23\,\mathrm{kg/m^3}$), both approximated to be spherical. Assuming a constant surface temperature of 205 K and $C_D = 2$, we find that γ is approximately 67 for single particles and at least 1.65 for agglomerates.

4. Discussion

It might be argued that our experiments simulate a rather simplistic comet, particularly in comparison to the KOSI experiments. However, our experiments address a few aspects of the physics of cometary activity that have received very limited attention to date.

4.1. Implication for comet models

Although the increase in hardness in our samples is not surprising, and matches Philae's measurements (Spohn et al., 2015),

its strong dependence on carbon content is probably a key observation of our experiments. In the physical system of our simulations, carbon is rather inert; it does not change any thermal or mechanical properties of the samples. Carbon does however change the absorption properties of the mixture in a fundamental way: up to 0.2%–0.3% carbon the hardness of a subsurface layer at 3–6 cm depth increases. Samples with a higher carbon content than 0.3% show less increase in mechanical hardness. We interpret this behaviour as follows: as the solar energy impinges on the sample, sublimation takes place not only on the surface but in a layer below the surface depending on the translucence of the sample. While the water vapour released at the surface is directly released into free space, the vapour molecules in the underlying layers travel along the vapour pressure gradient, i.e. down towards the cooler base plate, and are deposited as the temperature decreases with depth, thus increasing the hardness of the ice in a layer 3–6 cm below the surface. Increased carbon content results in increased absorption of 'solar' energy at depth and thus higher ice sublimation rates, which is why hardness increases. Once a threshold (around 0.2%–0.3%) is exceeded, the embedded carbon particles dominate light absorption to the extent that only very little sunlight can penetrate deep enough into the subsurface to sublime sufficient amounts of water ice to cause substantial subsurface hardening; most sunlight is absorbed at the surface and the vapour escapes. This result shows that many comet models which treat the nucleus surface as a two-dimensional plane where gas production takes place are probably somewhat over-simplistic. If our simple experiments show such a drastic difference in hardness then clearly, solar absorption at depth must play an important role in the physical evolution of the near-surface ice of a nucleus.

4.2. Possible interpretation of spacecraft observations

Our experiments offer a few more, albeit somewhat speculative, hints at what Rosetta and other comet missions observed. In our experiments, the hardened subsurface layer is found a few cm below the surface because the thermal gradient, at tens of K over 10 cm, is very steep. In nature, the subsurface thermal gradient of a nucleus is going to be a small fraction of this (see, e.g., Kossacki et al., 2015). As a result, we can expect such a hardened layer to occur several m or tens of m below the surface. Over time, even an initially homogeneous nucleus would become stratified in terms of mechanical strength. We can speculate about a possible stratification mechanism driven by the interplay of different sublimation temperatures of volatile constituents such as water, CO2, CO, methane and ammonia, which would all condense at different depths. Such a stratigraphy might have to do with Rosetta's observations of plate- or layer-like surface features such as smooth-floored pits on 67P, which are reminiscent of an onion skin-like structure.

Although the gravity is 3 to 4 orders of magnitude higher on Earth than on a comet (67P: $g = 2e\text{-}4\ m/s^2$, Groussin et al., 2015), some dust/gas jets can be observed during the whole irradiation phase. Agglomerates of about 1 mm diameter can still be lifted from the surface reaching highs up to a few millimetre before they fall back at a different position on the surface. The lifting of dust leads to bright spots, where fresh sample ice is exposed, similar to the bright regions observed by Rosetta.

We are at a loss as to what makes the carbon agglomerates stick together. Initially we suspected that the UV part of the radiation may have triggered a photochemical reaction forming a simple organic adhesive. However, when we filtered the UV and repeated our experiments, we obtained the same, mechanically stable agglomerates.

A possible explanation might be found in the physics of asteroids. Scheeres et al. (2010) made a comparison of the different forces (gravitational and non-gravitational forces) that are relevant for regolith on the surfaces of small asteroids and found that cohesive forces may play an important role for these bodies. Based on this hypothesis, Sanchez and Scheeres (2014) generated a model that, due to small van der Waals forces between constituent grains, small rubble pile asteroids have a small but nonzero cohesive strength. They concluded that the finest grains within an asteroid can serve as some kind of glue, a cohesive matrix that binds larger boulders together.

If van der Waals forces can provide enough strength for these agglomerates that form parts of the sample crust to survive manhandling during collection, weighing and drying, then they might also play a role in holding the material ejected from of comets together.

It should be noted that our observations of agglomerated surface particles seem to match the observations of spacecraft experiments. For the Giotto mission, Simpson et al. (1987) reported clusters and packets of particles. Further evidence of large, 'fluffy' dust particles was found during the Stardust (Green et al., 2004) and Rosetta missions (Fulle et al., 2015). Possibly these are held together by the same glue or forces as our dust agglomerates.

5. Conclusions

Physical and chemical properties of the complex system that is a comet cannot be wholly explained by a simple series of experiments with ice and carbon dust. As explained by Keller and Markiewicz (1991), performing a real simulation of cometary surfaces on Earth is impossible and the application of laboratory results to a real comet is never straightforward. However, fundamental experiments can help understand some of the features observed on comets.

Subsurface hardening in cometary analogues has been verified in experiments in the past (see e.g. Kochan et al., 1989, Kossacki et al., 1997). All samples investigated by Kochan et al., included CO_2 ice. The dimensions of the small KOSI chamber and the pressure were similar to ours, although our sample was more than twice as high. They radiated the samples for a much shorter time (~2–3 hours) but with higher intensity (2–2.4 SC). What our experiments have highlighted is the critical dependence of subsurface vapour activity on subsurface light absorption. In all our experiments the same power density is available. Nevertheless, the evolution of the sample critically depends on where the solar energy is absorbed: at or below the surface.

Our experiments also produced large, low-density dust aggregates from pure carbon particles. The mechanical strength of these aggregates is sufficient for them to survive collection and weighing.

Finally, it has to be stressed that we have produced a low-albedo dust mantle with active surface regions from an ice-dust mixture with an extremely low proportion of dust. This suggests caution when quantifying the bulk ratio of ice to refractory components of a real comet nucleus from remote observations alone.

Acknowledgements

This project is funded by STFC under grant number ST/P000657/1. The authors would like to thank Oliver Grabowski for his help with the realization of the hardness measurements. This paper was significantly improved thanks to the helpful comments of two anonymous reviewers.

References

Barucci, M.A., et al., 2016. Detection of exposed H_2O ice on the nucleus of comet 67P/Churyumov-Gerasimenko as observed by Rosetta OSIRIS and VIRTIS instruments. Astron. Astrophys. 595 (A102), 13. doi:10.1051/0004-6361/201628764.

Benkhoff, J., Spohn, T., 1991. Results of a coupled heat and mass transfer model applied to KOSI sublimation experiments. In: Kömle, N.I., Bauer, S.J., Spohn, T. (Eds.), *Theoretical Modelling of Comet Simulation Experiments*, Proceedings of the KOSI modeller's workshop, 4-5 October 1990 in Graz. Verlag der Österreichischen Akademie der Wissenschaftern, pp. 31–47.

Birch, S.P.D., 2017. Geomorphology of comet 67P/Churyumov–Gerasimenko. MNRAS 469 (Issue Suppl_2), S50–S67 21 July 2017.

Brown, R.H., Lauretta, D.S., Schmidt, B., Moores, J., 2012. Experimental and theoretical simulations of ice sublimation with implications for the chemical, isotopic, and physical evolution of icy objects. Planet. Space Sci. 60, 166. doi:10.1016/j.pss.2011.07.023.

Coradini, A., et al., 2007. Virtis: an imaging spectrometer for the Rosetta Mission. Space Sci. Rev. 128 (1-4), 529–559. doi:10.1007/s11214-006-9127-5.

El-Maarry, M.R., et al., 2015. Regional surface morphology of comet 67P/Churyumov-Gerasimenko from Rosetta/OSIRIS images. Astron. Astrophys. 583, A26. doi:10.1051/0004-6361/201525723.

Epifanov, V.P., 2004. Rupture and dynamic hardness of ice. Dokl. Phys. 49 (2), 86–89. doi:10.1134/1.1686876.

Fulle, M., et al., 2015. Density and charge of Pristine Fluffy Particles from comet 67P/Churyumov-Gerasimenko. Astrophys. J. Lett. 802 (1), L12. doi:10.1088/2041-8205/802/1/L12.

Green, S.F., et al., 2004. The dust mass distribution of comet 81P/Wild 2. J. Geophys. Res. 109 (E12), E12S04. doi:10.1029/2004JE002318.

Groussin, O., et al., 2015. Gravitational slopes, geomorphology, and material strengths of the nucleus of comet 67P/Churyumov-Gerasimenko from OSIRIS observations. Astron. Astrophys. 583, A32. doi:10.1051/0004-6361/201527020.

Grün, E., et al., 1993. Development of a dust mantle on the surface of an insolated ice-dust mixture - results from the KOSI-9 experiment. J. Geophys. Res. 98 (E8). doi:10.1029/93JE01134, (ISSN 0148-0227)15,091-15,104.

Gundlach, B., Skorov, Yu.V., Blum, J., 2011. Outgassing of icy bodies in the Solar System – I. The sublimation of hexagonal water ice through dust layers. Icarus 213 (2), 710–719. doi:10.1016/j.icarus.2011.03.022.

Keller, H.U., Markiewic, W.J., 1991. KOSI? Geophys. Res. Lett. 18 (2), 9–252. doi:10.1029/90GL02591.

Keller, H.U., et al., 2007. OSIRIS: the scientific camera system onboard Rosetta. Space Sci. Rev. 128 (1-4), 433–506. doi:10.1007/s11214-006-9128-4.

Kochan, H., Roessler, K., Ratke, L., Heyl, M., Hellman, H., Schwehm, G., 1989. Crustal strength of different model comet materials. In: ESA, *Physics and Mechanics of Cometary Materials*, pp. 115–119. (SEE N90-19989 12-90).

Kochan, H.W., Huebner, W.F., Sears, D.W.G, 1998. Simulation experiments with cometary analogous material. Earth, Moon, and Planets 80 (1/3), 369–411. doi:10.1023/A:1006342602452.

Kömle, N.I., Kargl, G., Thiel, K., Seiferlin, K., 1996. Thermal properties of cometary ices and sublimation residua including organics. Planet. Space Sci. 44, 675. doi:10.1016/0032-0633(96)00043-8.

Kossacki, K.J., Kömle, N.I., Leliwa-Kopystynski, J., 1997. Laboratory investigation of the evolution of cometary analogs: results and interpretation. Icarus 128, 127–144. doi:10.1006/icar.1997.5701.

Kossacki, K.J., Leliwa-Kopystynski, J., 2014. Temperature dependence of the sublimation rate of water ice: influence of impurities. Icarus 233, 101. doi:10.1016/j.icarus.2014.01.025.

Kossacki, K.J., Spohn, T., Hagermann, A., Kaufmann, E., Kührt, E., 2015. Comet 67P/Churyumov-Gerasimenko: hardening of the sub-surface layer. Icarus 260, 464–474. doi:10.1016/j.icarus.2015.07.024.

Lämmerzahl, P., Gebhard, J., Grün, E., Klees, G., 1995. Gas release from ice/dust mixtures: results from eleven KOSI experiments. Planet. Space Sci. 43, 363–373. doi:10.1016/0032-0633(94)00121-7.

Li, J.-Y., et al., 2013. Photometric properties of the nucleus of Comet 103P/Hartley 2. Icarus 222, 559. doi:10.1016/j.icarus.2012.11.001.

Markiewicz, M.J., Kochan, H., Keller, H.U., 1991. Gas-particle interaction in KOSI cometary simulations. In: Kömle, N.I., Bauer, S.J., Spohn, T. (Eds.), *Theoretical Modelling of Comet Simulation Experiments*, Proceedings of the KOSI modeller's workshop, 4-5 October 1990 in Graz. Verlag der Österreichischen Akademie der Wissenschaftern, pp. 77–90.

Poch, O., Pommerol, A., Jost, B., Carrasco, N., Szopa, C., Thomas, N., 2016. Sublimation of water ice mixed with silicates and tholins: evolution of surface texture and reflectance spectra, with implications for comets. Icarus 267, 154–173. doi:10.1016/j.icarus.2015.12.017.

Poirier, L., Lozowski, E.P., Thompson, R.I., 2011. Ice hardness in winter sports. Cold Reg. Sci. Technol. 67, 129–134.

Pomeroy, J.W., Brun, E., 2001. Physical properties of snow. In: Jones, H.G., Pomeroy, J.W., Walker, D.A., Hoham, R.W. (Eds.), Snow Ecology -An Interdisciplinary Examination of Snow-Covered Ecosystems. Cambridge University Press, pp. 45–126.

Pommerol, A., Thomas, N., Affolter, M., Portyankina, G., Jost, B., Seiferlin, K., Aye, K.-M., 2011. Photometry and bulk physical properties of Solar System surfaces icy analogs: The Planetary Ice Laboratory at University of Bern. Planet. Space Sci. 59 (13), 1601–1612. doi:10.1016/j.pss.2011.07.009.

Pommerol, A., et al., 2015. OSIRIS observations of meter-sized exposures of H_2O ice at the surface of 67P/Churyumov-Gerasimenko and interpretation using laboratory experiments. Astron. Astrophys. 583, A25. doi:10.1051/0004-6361/201525977.

Sánchez, P., Scheeres, D.J., 2014. The strength of regolith and rubble pile asteroids. Meteorit. Planet. Sci. 49 (5), 788–811. doi:10.1111/maps.12293.

Scheeres, D.J., Hartzell, C.M., Sánchez, P., Swift, M., 2010. Scaling forces to asteroid surfaces: the role of cohesion. Icarus 210 (2), 968–984. doi:10.1016/j.icarus.2010.07.009.

Sears, D.W.G., Kochan, H.W., Huebner, W.F., 1999. Invited review: laboratory simulation of the physical processes occurring on and near the surface of comet nuclei. Meteorit. Planet. Sci. 34 (4), 497–525. doi:10.1111/j.1945-5100.1999.tb01360.x.

Sierks, H., et al., 2015. On the nucleus structure and activity of comet 67P/Churyumov-Gerasimenko. Science 347, 6220. doi:10.1126/science.aaa1044, aaa1044.

Simpson, J.A., Rabinowitz, D., Tuzzolino, A.J., Ksanfomaliti, L.V., Sagdeev, R.Z., 1987. The dust coma of comet P/Halley - measurements on the Vega-1 and Vega-2 spacecraft. Astron. Astrophys. 187 (1-2), 742–752.

Sunshine, J.M., et al., 2006. Exposed water ice deposits on the surface of Comet 9P/Tempel 1. Science 311 (5766), 1453–1455. doi:10.1126/science.1123632.

Spohn, T., et al., 2015. Thermal and mechanical properties of the near-surface layers of comet 67P/Churyumov-Gerasimenko. Science 349 (6247), aab0464. doi:10.1126/science.aab0464.

Steiner, G., Kömle, N.I., Kuehrt, E., 1991. Thermal modelling of comet simulation experiments. In: Kömle, N.I., Bauer, S.J., Spohn, T. (Eds.), *Theoretical Modelling of Comet Simulation Experiments*, Proceedings of the KOSI modeller's workshop, 4-5 October 1990 in Graz. Verlag der Österreichischen Akademie der Wissenschaftern, pp. 11–30.

Thomas, N., et al., 2015. Redistribution of particles across the nucleus of comet 67P/Churyumov-Gerasimenko. Astron. Astrophys. 583, A17. doi:10.1051/0004-6361/201526049.